

S(+)-4-(1-Phenylethylamino)quinazolines as Inhibitors of Human Immunoglobulin E Synthesis: Potency Is Dictated by Stereochemistry and Atomic Point Charges at N-1

Michael Berger,[†] Bettina Albrecht, Attila Berces, Peter Ettmayer,* Wolfgang Neruda, and Maximilian Woisetschlager

Novartis Forschungsinstitut, Brunnerstrasse 59, Vienna A-1235, Austria

Received March 30, 2001

Since the pathogenesis of allergic diseases is associated with elevated levels of immunoglobulin E (IgE), we developed a high throughput reporter gene assay in a human B-cell line to screen for low molecular weight IgE inhibitory compounds. Monitoring the IL-4 driven IgE-germline promoter activity (IgE-GLP), we discovered 4-(1-phenylethylamino)quinazolines as potent inhibitors of IgE-germline gene expression. Testing of the individual enantiomers (**1**, **2**) revealed that only the *S*(+) enantiomer **1** was active. A cell viability assay done in the same cell line in parallel discriminated the dose-dependent inhibition from a general antiproliferative effect. The observed correlation of the inhibitory potencies found in the reporter gene assay with those measured by IgE-ELISA in primary human splenocytes provided evidence that the blockade of IgE synthesis is the direct consequence of IgE-germline gene inhibition, thereby validating the reporter gene assay. Parallel synthesis in solution rapidly provided a series of analogues of compound **1** with modifications in the phenethylamine side chain and the quinazoline core for SAR studies. Increasing the lipophilicity of the arylalkylamine moiety yielded *S*(+)-4-(1-(2-naphthyl)ethylamino)quinazoline (**6**) as the most potent inhibitor (IC₅₀ of 14 nM) while the *R*(-) enantiomer was again found to be inactive. Within the set of *S* enantiomers, quantum mechanical calculations revealed that the IgE inhibitory activity can be quantitatively described by the charge at N-1 of the heterocyclic core and to a lesser extent by the molar refractivity. These results demonstrate the importance of electron-deficient fused 4-aminopyrimidines and lipophilic side chains for biological activity. The strong preference for the *S* configuration of the phenethylamine side chain is remarkable insofar as biological activity for fused 4-(1-phenylethylamino)pyrimidines has been published for the *R* enantiomers only (EGFR tyrosine kinase inhibition).

Introduction

The pathogenesis of allergic diseases such as atopic dermatitis (AD), allergic asthma, and allergic rhinitis is associated with elevated levels of immunoglobulin E (IgE). IgE binds to its high-affinity receptor FcεRI, which is expressed on mast cells, basophils, monocytes,¹ and Langerhans cells,² or to FcεRII (CD23) found on B-cells, monocytes, and dendritic cells.³ Interaction of allergens with IgE/FcεRI complexes on mast cells and basophils leads to receptor cross-linking and degranulation of these cells as measured by the release of pharmacological mediators (e.g., histamine, cytokines, and chemokines) responsible for the pathogenesis of allergic diseases.⁴ Recent studies established the involvement of IgE/allergen immune complexes in the enhancement and redirection of IgE-mediated allergen presentation,⁵ leading to the perpetuation and worsening of allergic conditions. Therefore, IgE appears to be critically involved in both immediate early and later chronic manifestations of the allergic immune response.

On the basis of the central role of IgE in allergic diseases, a number of strategies were developed either

to interfere with its production or to block its function. Both approaches provided proof of concept that inhibition of IgE has therapeutic effects in animal models and in allergic patients. The small molecular weight compound suplatast tosylate has been described as an inhibitor of IL-4 and IL-6 production in T-cells, thereby leading to IgE inhibition in B-lymphocytes. In allergic patients, the drug improved clinical symptoms, which correlated with a decrease in serum IgE antibody levels.⁶ Soluble IL-4 receptor⁷ and mutant IL-4 proteins⁸ were shown to block IgE production, resulting in the inhibition of IgE-mediated allergic reactions.⁹ To interfere with the function of IgE, humanized non-anaphylactogenic anti-IgE antibodies such as rhuMAb-E25 are currently in clinical development. These antibodies interfered with virtually all aspects of IgE function in vitro and in vivo and had therapeutic effects in patients with allergic asthma and allergic rhinitis due to their selective neutralization and inhibition of IgE.¹⁰

On the basis of this evidence, it can be anticipated that a specific low molecular weight inhibitor of IgE synthesis in B-lymphocytes will have similar therapeutic effects in allergic patients with the advantages of an orally available drug. So far, there is no such drug on the market or in clinical development.

Searching for such low molecular weight inhibitors, we developed a high-throughput screening reporter gene

* To whom correspondence should be addressed. Phone: +43-1-86634-9038. Fax: +43-1-86634-582. E-mail: peter.ettmayer@pharma.novartis.com.

[†] Current address: Intervet, Althanstrasse 14, Vienna A-1090, Austria.

assay in a human B-cell line monitoring early steps of IgE isotype switching. The screening for compounds that interfered with the IL-4 and anti-CD40 mAb induced IgE-germline promoter activity but not with cell viability led to identification of (*S*)-4-(1-phenylethylamino)quinazoline as a potent and selective inhibitor. The inhibitory potencies measured in the reporter gene assay for both enantiomers correlated with the inhibition of IgE synthesis in primary human splenocytes, thereby validating the HTS assay. Parallel synthesis in solution utilizing polymer-supported quenching reagents provided a series of analogues of compound **1** for SAR studies. Here, we report the effect of the stereochemistry in the phenethylamine side chain and the charge properties of the heterocyclic core of fused 4-(1-phenylethylamino)pyrimidines on the inhibition of the IgE-germline promoter activity.

Biology

IgE is produced by a subset of B-lymphocytes that are generated during an allergic immune response as the result of IgE isotype switching. This differentiation process is driven by direct contact of the B-cells with activated T-helper (T_H) cells and by T_H -cell-derived interleukin-4 (IL-4) or IL-13. IL-4 induces transcription from the IgE-germline promoter (IgE-GLP) through the ϵ -switch region and the C_ϵ gene locus. This activation is essential and primes the B-cells for the subsequent DNA switch recombination step, which is mainly driven by signals originating from the T/B-cell contact, such as the interaction of the T_H -cell-expressed CD40 ligand with its CD40 receptor on B-cells. The recombined genome allows for the generation of productive IgE transcripts and the synthesis and secretion of IgE protein.¹¹ In cell culture systems, T/B cell contact can be mimicked by cultivation of primary B-cells with agonistic anti-CD40 monoclonal antibodies. Thus, a blockade of the IL-4 induced activity of the IgE-GLP should result in diminished IgE isotype switching and IgE synthesis. To be able to screen for inhibitors of IgE-GLP activation, a reporter gene assay was developed. The human B-cell line BL2 was stably transfected with a plasmid in which the luciferase reporter gene is under the control of a 630 bp fragment encompassing all regulatory DNA elements known to be involved in the IL-4 response.¹² The cytokine inducibility of the luciferase gene was compared with the one of the endogenous IgE-germline gene. Figure 1A demonstrates that IL-4 led to a ca. 7-fold induction of luciferase expression, while stimulation with anti-CD40 mAb had no effect. The combination of the two reagents acted synergistically to achieve a 35-fold up-regulation of reporter gene expression. Synergy of the IL-4 and CD40 mediated induction of IgE-GLP activity has been shown before in primary human B-cells.¹³ Essentially the same results were obtained when steady-state levels of IgE-germline transcripts were quantitated in the same cells (Figure 1B). From that we conclude that this reporter gene assay closely mimics the situation seen during the early steps in IgE isotype switching and thus is useful for screening for inhibitors. B-cell viability, as determined by mitochondrial activity, was assessed in parallel to discriminate from general antiproliferative effects.

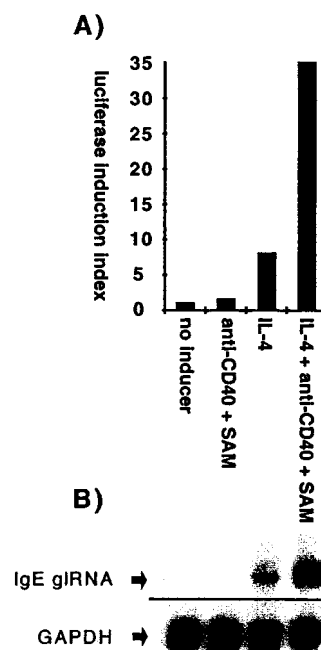


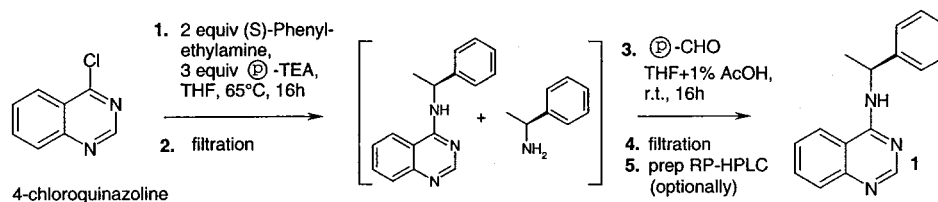
Figure 1. Comparison of the cytokine inducibility of the luciferase gene and the endogenous IgE-germline gene. Transfectant cells were stimulated with IL-4, anti-CD40 monoclonal antibodies (mAb), or both for 24 h. The antibodies were cross-linked with sheep antimouse IgG antibodies (SAM) to mimic the trimeric conformation of the natural ligand for CD40. Induced IgE-GLP activity was assessed either by luciferase assays for the transgene promoter or by detection of IgE-germline transcripts (IgE gRNA) for the endogenous promoter.

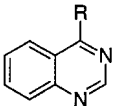
Chemistry

The 4-aminopyrimidines were prepared by parallel synthesis in solution, utilizing polymer-supported quenching reagents.¹⁴ The substituted 4-chloropyrimidines were reacted with 2 equiv of amines in the presence of polymer-supported triethylamine (P-TEA , Scheme 1) to achieve complete turnover. Because of the different reactivity of the educts, the reactions had to be divided into three sets: (A) reaction in THF at 65 °C for 16 h (**1–15**); (B) DMF/*n*-butanol, 100 °C, 16 h (**16–18**, **20**, **23–30**); and (C) neat, 160 °C, 1 h (**19**, **21**, **22**) (Tables 1 and 2). After filtration the reaction mixtures were incubated with Wang aldehyde resin¹⁵ (P-CHO) in tetrahydrofuran containing 1% of acetic acid for 16 h at room temperature to remove excess of amine by Schiff base formation. The catalytic amount of acetic acid was found to be essential for complete removal of the primary amine in the presence of the secondary amine in the product. Acidic ion-exchange resin also tended to bind the product. Removal of the solvents provided the final product in near-quantitative yield and greater than 90% purity. Further purification was done by crystallization (**1–5**, **19**, **22**) or by automated preparative HPLC on reversed phase using water/acetonitrile gradients containing 0.1% TFA (**6–13**, **16–18**, **20**, **21**, **24–25**). The latter compounds were tested as their TFA salts. Purity and homogeneity of the final compounds were assessed by RP-HPLC, TLC, and ^1H NMR spectroscopy.

Results and Discussion

Screening for inhibitors of IL-4/anti-CD40 mAb induced IgE-germline promoter activation revealed race-

Scheme 1. Representative Example of the Parallel Synthesis Scheme in Solution Utilizing Polymer-Supported Quenching Reagents**Table 1.** Variation in the Side Chain of 4-(1-Phenylethylamino)quinazolines

 1-17									
R	method	yield ^a (%)	purity ^b (%)	mp (°C)	[α] _D ²⁰ (deg)	MW	MH ⁺ (ESI, m/z)	IgE-GLP-RGA, IC ₅₀ ± SEM (n) ^d	CellProl_XTT, IC ₅₀ ± SEM (n) ^d
1 (S)-1-phenylethylamine	A	55	99.6	123–124	+169.1	249.3	250.1	127 ± 14 (19)	>2000 (4)
2 (R)-1-phenylethylamine	A	67	100	123–124	–168.5	249.3	250.1	>2000 (4)	>2000 (3)
3 benzylamine	A	66	100	171		235.3	236.0	>2000 (4)	>2000 (3)
4 (S)-1-cyclohexylethylamine	A	76	100	167–168	+124.5	255.4	256.1	81 ± 9 (5)	>2000 (3)
5 (R)-1-cyclohexylethylamine	A	71	100	167–168	–128.7	255.4	256.0	>2000 (3)	>2000 (3)
6 (S)-1-(2-naphthyl)ethylamine	A	80	100		+199.6	299.4 + 114	300.1	14 ± 3 (5)	1633 ± 300 (3)
7 (R)-1-(2-naphthyl)ethylamine	A	60	100		–199.4	299.4 + 114	300.0	>2000 (2)	>2000 (2)
8 (S)-1-(4-bromophenyl)ethylamine	A	68.7	100			328.2 + 114	328.0	72 ± 14 (4)	>2000 (2)
9 (S)-1-(4-methylphenyl)ethylamine	A	74.6	95.8			263.3 + 114	264.1	46 ± 7 (4)	>2000
10 (S)-1-(4-methoxyphenyl)ethylamine	A	75	95.8			279.3 + 114	280.1	45 ± 8 (4)	>2000 (2)
11 (S)-1-(3-methoxyphenyl)ethylamine	A	81	94.8			279.3 + 114	280.1	23 ± 3 (4)	>2000
12 (S)-1-phenylpropylamine	A	58	99.6			263.3 + 114	264.1	147 ± 25 (5)	>2000 (3)
13 (S)-1-2-amino-2-phenylethanol	A	72.9	98.7			265.3 + 114	266.0	149 ± 88 (5)	>2000 (3)
14 (S)-1-aminoindane	A	64	94.7		+ 4.0	261.3	262.0	>2000 (4)	>2000 (3)
15 (R)-1-aminoindane	A	80	94.7		–2.1	261.3	262.0	1015 ± 212 (4)	>2000 (3)
16 N-methyl-1-phenylethylamine	B	99	99.4			263.3 + 114	264.0	>2000 (2)	>2000 (2)
17 anilin	B	61	97.9			221.3 + 114	222.0	>2000 (2)	>2000 (2)

^a Isolated yields after purification (recrystallization or preparative HPLC). ^b Purity of the final products by HPLC, 254 nm. ^c Determined in ethanol, c = 1 g/100 mL. ^d Mean values from *n* independent IC₅₀ determinations (in nM) are given ± the standard error.

Table 2. Variation in the Heterocyclic Core of (Fused) 4-(1-Phenylethylamino)pyrimidines

1, 18-30

	R	method	yield ^a (%)	purity ^b (%)	mp (°C)	MW	MH ⁺ (ESI, <i>m/z</i>)	IgE-GLP–RGA, IC ₅₀ ± SEM (<i>n</i>) ^c	CellProl_XTT, IC ₅₀ ± SEM (<i>n</i>) ^c
1	quinazolin-4-yl	A	55	99.6	123–124	249.3		127 ± 14 (19)	>2000 (4)
18	6,7-dimethoxyquinazolin-4-yl	B	78	99.3		309.4 + 114	310.1	>2000 (2)	>2000 (2)
19	quinolin-4-yl	C	60	100	87–89	248.3	249.1	701 ± 87 (5)	>2000 (4)
20	7-chloroquinolin-4-yl	B	41	99.0		282.8 + 114	283.0	670 ± 123 (5)	>2000 (4)
21	2-methylquinolin-4-yl	C	71	99.2		262.4 + 114	263.1	>2000 (2)	>2000 (2)
22	isoquinolin-1-yl	C	33	99.3	80–81	248.3	249.1	>2000 (3)	>2000 (4)
23	2-methylthiopyrimidin-4-yl	B	31	99.4		245.3	246.0	931 ± 204 (3)	>2000 (3)
24	2-amino-6-methylpyrimidin-4-yl	B	27	95.2		228.3 + 114	229.1	>2000 (2)	>2000 (2)
25	6-methylpyrrolo[2,3- <i>d</i>]pyrimidin-4-yl	B	48	92.7		252.3 + 114	253.1	>2000 (2)	>2000 (2)
26	purin-6-yl	B	65	99.6		239.3	240.0	>2000 (2)	>2000 (2)
27	thieno[2,3- <i>d</i>]pyrimidin-4-yl	B	53	100		255.3	256.0	370 ± 70 (4)	>2000 (3)
28	5-methylthieno[2,3- <i>d</i>]pyrimidin-4-yl	B	37	91.5		269.4	270.0	130 ± 12 (5)	1476± 317 (4)
29	thieno[3,2- <i>d</i>]pyrimidin-4-yl	B	37	99.6		255.3	256.0	>2000 (2)	>2000 (2)
30	7-methylthieno[3,2- <i>d</i>]pyrimidin-4-yl	B	21	92.9		269.4	270.0	>2000 (2)	>2000 (2)

^a Isolated yields after purification (recrystallization or preparative HPLC). ^b Purity of the final products by HPLC, 254 nm. ^c Mean values from *n* independent IC₅₀ determinations (in nM) are given ± the standard error.

mic 4-(1-phenylethylamino)quinazoline as hit. To determine the role of the stereochemistry on the biological activity, the individual enantiomers **1** and **2** were synthesized and tested in the reporter gene assay (Table 1). Luciferase expression was blocked by the S(+) enantiomer **1** in a dose-dependent manner with an IC₅₀ of 125 nM (Figure 2), while the corresponding R(–) enantiomer **2** did not inhibit the IL4-driven germline promoter activity up to the highest concentration tested (2 μM). The viability of the B-cells, assessed in parallel,

was only effected at 20 times higher concentrations of compound **1** (IC₅₀ of 2.5 μM, Figure 2).

On the basis of the observed enantioselective inhibition in the reporter gene assay, compounds **1** and **2** qualified as tools to validate the concept that the blockade of IL-4-dependent IgE-germline gene transcription should lead to inhibition of IgE switch recombination and IgE secretion from B-cells. Human splenocytes were cultivated with IL-4 and agonistic anti-CD40 mAb in the presence of increasing concentrations

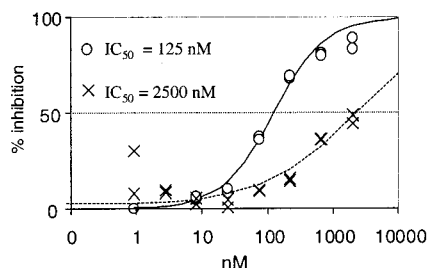


Figure 2. Inhibition of IgE-germline promoter activity in BL-2 cells by **1** (O, duplicates). Parallel cultures were quantitated for cell viability (X, duplicates) in the presence of **1**.

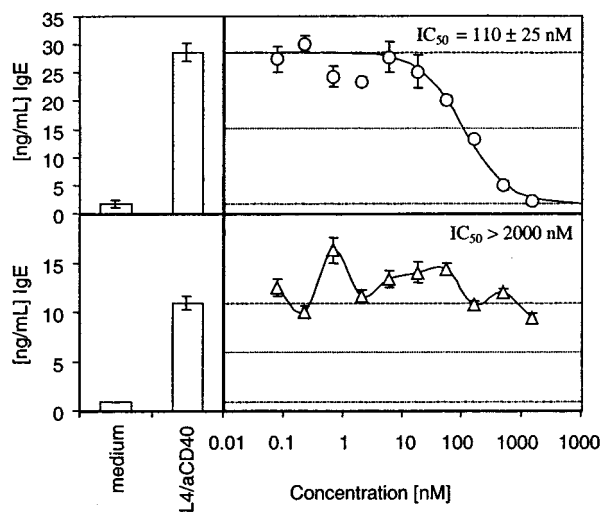


Figure 3. Dose-response curves of quinazolins **1** (O) and **2** (Δ) on IgE synthesis in human splenocytes. Data are presented as mean \pm SEM ($n = 4-12$).

of **1** or **2**. After 9 days, IgE was quantitated in the cell supernatants by ELISA. Figure 3 demonstrates that **1** but not **2** blocked IgE production in a dose-dependent manner. The IC_{50} value of 110 nM measured for **1** is very similar to the one calculated in the IgE-GLP reporter gene assay. From these data we conclude that the observed block in IgE synthesis is a direct consequence of inhibition of IgE-germline gene inhibition. Therefore, the basic concept could be validated and verified in relevant target cells.

To further substantiate the observed enantioselectivity for biological activity, the corresponding nonchiral 4-benzylquinazoline (**3**) and both enantiomers of the 4-(1-cyclohexylethyl)amino (**4/5**) and 4-(1-naphthylethyl)aminoquinazoline (**6/7**) were tested in the reporter gene assay (Table 1). Nonchiral **3** did not effect the IL-4 driven induction of the germline transcript up to 2000 nM, highlighting the importance of the α branching of the 4-amino substituent. When the 1-phenylethylamino group in **1** and **2** was replaced by the 1-cyclohexylethylamino group, the *S*(+) enantiomer (**4**) was found to 1.5 times more potent than **1** and more than 25 times more active than *R*(-)-**5**. Further enhancing the lipophilicity of the side chain by incorporation of (*S*)-1-(2-naphthyl)ethylamine yielded **6**, the most potent derivative within this series (IC_{50} of 14 nM). The *R*(-) enantiomer **7** was again found to be inactive at the highest tested concentration (2 μ M). Bromo (**8**), methyl (**9**), and methoxy (**11**, **12**) substitutions on the phenylethylamine residue in **1** were also well tolerated, leading to 3–5 times increased potencies compared to **1**. Comparing the potencies of **11**

and **12** might indicate a preference for the meta substitution.

Replacing the (*S*)-1-phenylethylamino group in **1** with a (*S*)-1-phenylpropylamino moiety (**12**) or (*S*)-phenylalaninol (**13**) resulted in IC_{50} values comparable to that of **1**. Substantially decreased potency was observed when the 1-phenylpropylamino group in **12** was replaced with the 1-aminoindane moiety (**14**, **15**). Interestingly this time the *R* enantiomer **15** was found to have a weak biological activity (IC_{50} of 1015 nM) while the *S* enantiomer **14** was inactive up to 2 μ M. When the 4-amino group in quinazoline **1** was methylated (**16**), no inhibitory activity was observed up to the highest tested concentration. A similar loss of potency was observed when the 1-phenylethylamino moiety was replaced by aniline (**17**). Both findings highlight the importance of an α -branched, *S*-configured, lipophilic secondary amine in position 4 of the quinazoline for IgE inhibitory activity.

To establish the role of the quinazoline core of **1** in the IL-4 driven IgE-germline promoter inhibition, we studied a diverse set of substituted heterocycles, keeping the *S*-phenylethylamine side chain constant (Table 2, Figure 4). 6,7-Dimethoxy substitution on the quinazoline ring resulted in complete loss of potency (**18**). We also found that the nitrogen in position 3 of the quinazoline can be replaced by carbon but the resulting quinoline **19** is 5 times less active than the lead compound **1**. Substitution on the quinoline ring is tolerated in position 7 (Cl, **20**) and not allowed in position 2 (CH₃, **21**). Isoquinoline **22** (replacement of the nitrogen in position 1 by carbon) was found to be inactive. A similar observation as with the quinolines **20** and **21** was made for substituted pyrimidines **23** and **24**. While weak activity was measured for the 2-methylthiopyrimidine (**23**, IC_{50} of 931 nM), no activity was obtained for the 2-amino-6-methylpyrimidine derivative **24**. Replacing the benzene ring in the quinazoline core with pyrrole and imidazole yielded the pyrrolo[2,3-*d*]pyrimidine **25** and the purine derivative **26**, both being inactive up to 2 μ M. When the benzene ring was replaced by thiophene, only the thieno[2,3-*d*]pyrimidines **27** and **28** inhibited the IgE promoter activity with similar potencies as the lead compound **1**. The thieno-[3,2-*d*] pyrimidines (**29**, **30**) were inactive up to the highest tested concentration (2 μ M).

To better understand the structural properties that are beneficial for the inhibition of IgE synthesis within this compound class, besides the pronounced preference for the *S* enantiomers, we calculated several physicochemical properties for the *S* enantiomers (**1**, **4**, **6**, **8–14**, **18–30**) and compared them with the biological activity measured in the reporter gene assay. Interestingly, we discovered that the activity as plotted by $\log(IC_{50})$ correlated well with the charge at the N atom (Q_N) as shown in Figure 5. The atomic point charges were calculated by density functional quantum chemistry calculations as described in the Experimental Section under "Computational Details".

Classifying compounds **21** and **23** as outliers, the inverse correlation can be described by a linear correlation coefficient R of -0.94 . The pyrimidine **21** and the quinoline **22** are both less active than the point charge

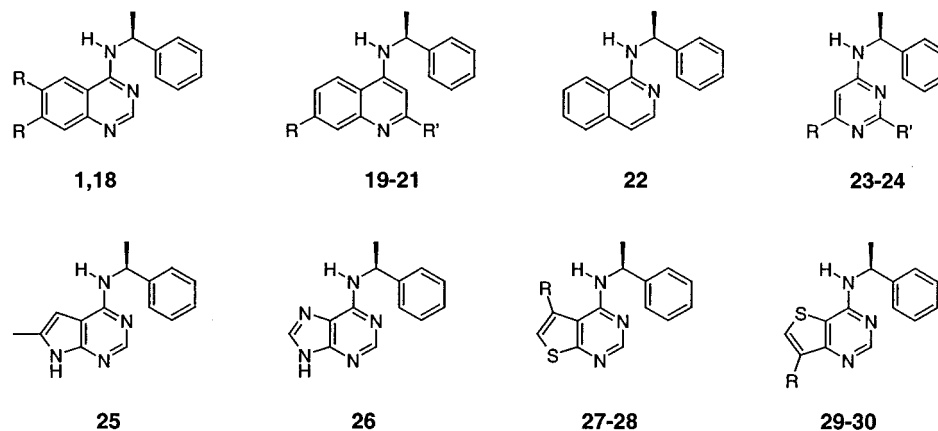


Figure 4. Modifications of the heterocyclic core of 4-(1-phenylethylamino)pyrimidines.

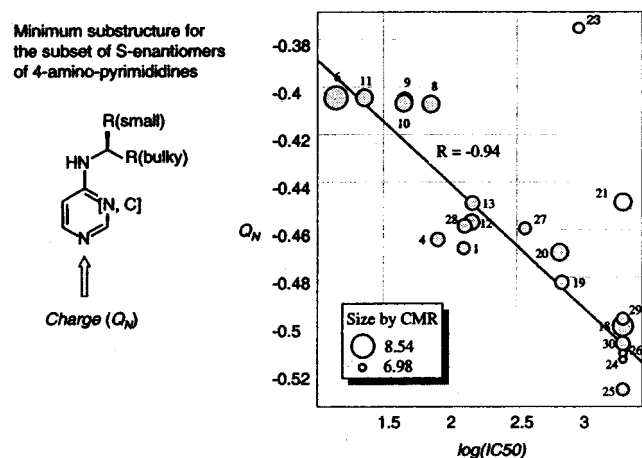


Figure 5. Correlation between the calculated point charge Q_N and $\log(\text{IC}_{50})$ for a subset of 4-aminopyrimidines. Filled circles were used in the R calculation and the straight line fit (—). Circles are labeled with the compound number.

would predict. It is interesting to note that both outliers are substituted at the 2 position, and the lack of potency could be attributed to unfavorable interaction of this position with the unknown receptor. Molar refractivity¹⁶ (polarizability) correlated to a lesser extent with $\log(\text{IC}_{50})$ (CMR, $R = -0.55$; the size of the circles plotted in Figure 5 corresponds to the CMR values), and there was a cross-correlation between CMR and Q_N with a correlation coefficient (R) of 0.60. No correlation of $\log(\text{IC}_{50})$ and CLOGP was observed ($R = -0.32$). On this basis, the activity can be well represented by only one parameter, the Q_N point charge, in the following equation:

$$\log(\text{IC}_{50}) = -5.33(\pm 0.70) - [16.75(\pm 1.50)]Q_N \quad (1)$$

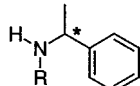
It is remarkable that within a range of 3 orders of magnitude the IC_{50} values of 19 out of 21 compounds fit the equation well (Figure 5). With the above density functional quantum chemistry calculations the lack of activity of the dimethoxy-substituted quinazoline **18** can be rationalized by the +M effect of the methoxy substitution increasing the negative charge Q_N at the N1 atom of the pyrimidine ring. The same argument provides a rationale for why the thieno[2,3-*d*]pyrimidines **27** and **28** are more active than the corresponding thieno[3,2-*d*]pyrimidines **29** and **30**. The +M effect of the S atom on C5 of the pyrimidine (**29**, **30**) donates

electrons to N1, whereas the S atom on C6 of the pyrimidines **27** and **28** lowers the negative charge on N1.

To evaluate the PK properties, compounds **4** and **5** were administered to mice orally (**4**, 30 mg/kg) and by intravenous injection (**4** and **5**, 10 mg/kg) for plasma level determination by LC-MS. After oral administration, plasma levels of **4** were below the detection limit. After intravenous administration, the $R(-)$ enantiomer **5** was found to be rapidly cleared from the system (10 mg/kg, $\text{AUC}_{0-5\text{h}}$ 0.92 $\mu\text{M h}$, Cl 43.6 [$\text{kg}^{-1} \text{h}^{-1}$]). Because of acute toxicity, no PK data could be obtained for the biologically active $S(+)$ enantiomer **4**.

Conclusions

$S(+)$ -4-(1-Arylethylamino)quinazolines were discovered as potent and enantioselective inhibitors of the IL4-driven IgE-germline promoter activity in human B-lymphocytes. A cell viability assay proved that the inhibition is not due to a general antiproliferative effect. The potencies found in the reporter gene assay could be correlated with those measured by IgE-ELISA in primary human splenocytes, thereby providing evidence that the block of IgE synthesis is the direct consequence of IgE-germline inhibition. Within the set of S enantiomers, quantum mechanical calculations revealed that the IgE inhibitory activity can be quantitatively described by the charge at N-1 of the heterocyclic core and to a lesser extent by the molar refractivity. These results show the importance of electron-deficient fused 4-aminopyrimidines and of lipophilic side chains for biological activity in addition to the strong preference for the S configuration of the phenethylamine side chain. The S -enantioselective inhibition is remarkable insofar as biological activity for fused 4-(1-phenylethylamino)pyrimidines has been published for the R enantiomers only. **2** was reported as an ATP site directed reversible inhibitor of the epidermal growth factor receptor (EGFR) tyrosine kinase (IC_{50} of 86nM), whereas the $S(+)$ enantiomer **1** shows no activity up to 10 μM in the EGFR assay.¹⁷ For the corresponding pyrido[5,4-*b*]indoles,¹⁸ benzothieno[2,3-*d*]pyrimidines¹⁸ and pyrrolo[2,3-*d*]pyrimidines,¹⁹ where data on EGFR tyrosine kinase inhibition is published, a similar preference for the R enantiomers is observed (Table 3). While the molecular target for the IgE-germline promoter inhibitors remains unknown, the potential correlation of the IgE inhibitory activity with the acute toxicity in mice could point

Table 3: Blockage of EGF-Stimulated Tyrosinephosphorylation in EGFR-Positive A 431 Cells


R	*	EGFR, IC ₅₀ (nM)	IgE-GLP-RGA, IC ₅₀ (nM)
quinazolin-4-yl	1	<i>S</i> >10 ⁴ ^a	127
quinazolin-4-yl	2	<i>R</i> 86 ^a	>2000
2,4,9-triazafluoren-1-yl		<i>S</i> >10 ⁵ ^b	
2,4,9-triazafluoren-1-yl		<i>R</i> 419 ^b	
benzothieno[3,2- <i>d</i>]-pyrimidin-4-yl		<i>R</i> 538 ^b	
6-phenylpyrrolo[2,3- <i>d</i>]-pyrimidin-4-yl		<i>R</i> 10–50 ^c	

^a IC₅₀ values as published in ref 17. ^b IC₅₀ value as published in ref 18. ^c IC₅₀ value as published in ref 19.

toward a common target. *N*-Alkyl-4-aminoquinazolines are reported to be the most potent synthetic inhibitors of the NADH-ubiquinone reductase activity of complex I (the function of the energy-conserving enzyme complex is particularly crucial in tissues such as neurons that heavily rely on mitochondrial ATP- and NAD-linked pathways).²⁰ Unfortunately, nothing is published about the enantioselectivity of complex I inhibition. The potential correlation between IgE inhibition in human splenocytes and complex I inhibition is the topic of ongoing investigations.

Experimental Section

Chemistry. Melting points were determined on a Neolab automated melting apparatus and are uncorrected. The ranges given reflect the results from two independent melts. ¹H and ¹³C NMR spectra were recorded on Bruker AC 250 or Avance 400 systems. Optical rotation data were obtained using a Perkin-Elmer model 241 polarimeter. Analytical HPLC analyses were performed on a HP 1100 system with a multiwavelength detector using a Waters Xterra column (4.6 mm × 50 mm C₁₈, 3.5 μm) and a flow rate of 2 mL/min. The column was eluted with a linear gradient of 10–95% acetonitrile in water containing 0.1% TFA in 6 min. Preparative HPLC separations were performed on a Gilson system (model 322 pump, model 215 liquid handler, model 155 dual-wavelength detector) using a Waters Prep Nova-Pak cartridge (25 mm × 100 mm C₁₈, 6 μm) and a flow rate of 25 mL/min. The column was eluted with a linear gradient of 10–90% acetonitrile in water containing 0.1% TFA in 13 min. MS analyses were obtained on a HP model 1100 system with direct flow injection into a Thermoquest (Finnigan) MS detector with electrospray ionization. Parallel syntheses were performed on a Quest 210 (Argonaut) in 5 mL reaction vessels or on a Tecan Combitec reaction block. Vacuum removal of solvents was achieved using an IR dancer (Hettlab) or a Genevac centrifuge. 4-Chloro-6,7-dimethoxyquinazoline, 4-chlorothieno[2,3-*d*]pyrimidine, 4-chloro-5-methylthieno[2,3-*d*]pyrimidine, 4-chlorothieno[3,2-*d*]pyrimidine, and 4-chloro-7-methylthieno[3,2-*d*]pyrimidine were purchased from Maybridge. 4-Chloroquinazolin²¹ and 4-chloro-6-methylpyrrolo[2,3-*d*]pyrimidine²² were prepared from their corresponding pyrimidinols.

General Method A. A reaction vessel for a Quest parallel synthesizer (5 mL) was charged with polymer-supported TEA (140 mg; diethylaminomethylpolystyrene, Fluka, 3.2 mmol/g, 0.45 mmol) and purged with argon for 10 min. 4-Chloroquinazoline (24.7 mg, 0.15 mmol) dissolved in THF (1 mL, 0.15 mM) was added followed by the corresponding amine (0.3 mmol) dissolved in THF (1 mL, 0.3 mM). The suspension was then agitated at 65 °C for 16 h. After cooling to room temperature, the mixture was filtered, the resin was washed with THF (2 × 2 mL), and the filtrates were combined in scintillation vials. ©-CHO was added (180 mg, Aldehyde Wang

resin, Novabiochem, 2.66 mmol/g, 0.5 mmol) together with acetic acid (70 μL). The mixture was agitated on an orbital shaker overnight and filtered, and the resin was washed with THF (2 × 2 mL). After removal of the solvent in vacuo the product was obtained in typically around 90% purity and near-quantitative yield and could be further purified by preparative HPLC.

General Method B. A reaction vial (10 mL) was charged with polymer-supported TEA (140 mg, diethylaminomethylpolystyrene, Fluka, 3.2 mmol/g, 0.45 mmol) and purged with argon for 10 min. 4-Chloropyrimidine or a 4-chloroquinazoline derivative (0.15 mmol) dissolved in DMF (0.6 mL) was added followed by a solution of the corresponding amine in 1-butanol (0.5 M, 0.6 mL). Subsequently 1-butanol (1.8 mL) was added and the suspension was agitated at 100 °C for 16 h. After cooling to room temperature, the mixture was filtered, the resin was washed with DMF (2 × 2 mL), and the filtrates were combined in scintillation vials. The solvent was removed in vacuo and the residue dissolved in THF containing 0.1% acetic acid (4 mL) and treated with ©-CHO as described in general method A.

General Method C. A V-bottom-shaped reaction vial (1 mL) was charged with 4-chlorochinolin (0.3 mmol) or a 1-chloroisochinolin derivative (0.3 mmol). The corresponding amine (0.6 mmol) was added, and the mixture was heated to 160 °C for 60 min. After cooling to room temperature, the resulting mixture was dissolved in DMF and purified by preparative HPLC.

Computational Details. The lowest energy conformation was searched by systematic bond rotation and the geometry optimized corresponding to the potential described in Merck Molecular Force Field (1994).²³ Subsequently, the electronic structure was calculated at the level of gradient-corrected density functional theory as implemented in the Jaguar²⁴ quantum chemistry program. The exchange–correlation functional included the Xα exchange potential by Slater²⁵ and the local correlation of Vosko, Wilk, and Nusair (VWN)²⁶ as well as self-consistent gradient corrections by Becke (1988)²⁷ and Perdew (1986)²⁸ for exchange and correlation, respectively. The basis set was 6-31G**. Atomic point charges were calculated by the Mulliken population analysis.²⁹ This fairly high level of theory may not be necessary for QSAR calculations. However, we found that for systems where electronic structure plays an important role in the activity relationship, the higher level of theory pays off by providing a better correlation. In addition, even these high-level calculations require only 20 min/molecule on a Silicon Graphics Origin 2000 workstation.

Biology. 1. Cell Culture and Reagents. The Epstein–Barr virus negative Burkitt's lymphoma B-cell line BL2 was carried in Yssel's medium (25) supplemented with 10% heat-inactivated fetal calf serum (GIBCO Laboratories, Grand Island, NY), 100 U/mL penicillin, and 100 μg/mL streptomycin. Cells were kept at 37 °C with 5% CO₂. Purified human recombinant IL4 was obtained from Novartis AG (Basle, CH) with a specific activity of 0.5 U/ng. The hybridoma cell line producing mouse monoclonal antihuman CD40 antibodies was obtained from Dr. Shu man Fu, University of Virginia, Charlottesville, VA.

2. RNA isolation and Northern blot analysis. Total RNA was isolated from cells by the RNazol method (Biotecx Laboratories, Inc., Houston, TX) according to the instructions of the manufacturer. Aliquots (15 μg) were subjected to electrophoresis in a 1.2% denaturing agarose gel and transferred to a nylon membrane (GeneScreen, DuPont, Boston, MA). The membranes were stained with 0.04% methylene blue in 0.5 M sodium acetate (pH = 5.2) for 10 min at room temperature followed by several washes in water to localize and quantify rRNA before hybridization. The RNA was hybridized at 65 °C to a ³²P-labeled oligonucleotide probe derived from the C₁ exon (5'-gccacagcggtgaacatctgctt-3'), which was labeled at the 3' end using the terminal transferase kit (Roche). The blots were washed for 30 min at 62 °C in wash mix 1 (3 × SSC, 5% SDS, 100 mM Na₂PO₄, pH = 7.0, 10 × Denhardt solution) followed by a short wash in 1 × SSC, 1%

SDS at 62 °C. Specific signals were visualized by exposure to X-ray films (Kodak BioMax MR) for 3 days. Then the blot was stripped and reprobed with a ³²P-labeled oligonucleotide probe specific for the glyceraldehyde-3-phosphate dehydrogenase (GAPDH) gene as control.

3. Induction of IgE Synthesis in Human Splenocytes. Normal human splenocytes were seeded at 1×10^5 cells/mL in 96-well round-bottom plates and cultivated with 50 ng/mL IL-4 and 1 μ g/mL anti-CD40mAb for 9 days. Compounds were dissolved in DMSO, diluted to suitable concentrations with culture medium, and added to the cells 2 h before the inducers. Supernatants from nine identical culture wells were pooled into three replicates, and IgE was quantitated by isotype-specific ELISA. Half-maximal inhibition was calculated using Origin 6.0 logistic fit.

4. Generation of Stable Reporter Gene Transfectants and Luciferase Assays. A 630 bp DNA fragment encompassing all relevant regulatory elements¹² of the human IgE-germline promoter was cloned into the vector pGL2-basic (Promega, Wisconsin, WI) in which a neomycin gene resistance cassette had been incorporated. BL2 cells were transfected by electroporation, and stable clones were selected in 1.8 mg/mL G418 (Gibco). Functional clones were further selected by induction with IL-4 and anti-CD40mAb for 48 h. The best responder clone was seeded at 1×10^6 cells/mL in a 96-well plate and induced for 48 h with 10 ng/mL IL-4, 1 μ g/mL anti-CD40mAb, and 1 μ g/mL sheep antimouse IgG (Grub, Vienna) to cross-link the CD40 antibodies. Then the cells were lysed and luciferase activity was determined, according to the instructions of the manufacturer, using the dual-luciferase reporter assay system (Promega). In parallel cultures, cell viability was quantitated as assessed by intact mitochondria (EZ4U, Biomedica, Vienna, Austria). In both assays, duplicates were analyzed. Half-maximal inhibition was calculated using Origin 6.0 logistic fit.

5. Pharmacology. For po administration the compounds were dissolved in ethanol/Labrafil M2125/corn oil, 150:350:500 w/w/w. The solutions were diluted with an equal part of isotonic glucose solution immediately before use. For intravenous administration the compounds were dissolved in Cremophor EL/ethanol, 3:1 w/w, and diluted with nine parts of isotonic glucose solution before use. Fasted female mice (strain Balb/c) were dosed with the compounds either perorally (po) per gavage or intravenously (iv) by injection into the tail vein. Blood samples were collected from three animals at six time points. Plasma was prepared from heparin-stabilized blood by centrifugation and stored at -20 °C until analysis. Analysis was done after protein precipitation using methanol followed by centrifugation on a HP1090 chromatograph equipped with a Merck Superspher RP 8 column.

Acknowledgment. The authors are grateful to Peter Nussbaumer for helpful discussions and a critical review of the manuscript. We thank Heinrich Aschauer for the pharmacokinetic studies and Elena Macoratti for technical assistance.

Supporting Information Available: ¹H NMR and ¹³C NMR data for all new compounds (4–6, 14–16, 19–21, 23–25, 28–30). This material is available free of charge via the Internet at <http://pubs.acs.org>.

References

- Maurer, D.; Fiebiger, E.; Reininger, B.; Wolff-Winiski, B.; Jouvin, M. H.; Kilgus, O.; Kinet, J. P.; Stingl, G. Expression of functional high affinity immunoglobulin E receptors (Fc epsilon RI) on monocytes of atopic individuals. *J. Exp. Med.* **1994**, *179*, 745–750.
- Reischl, I. G.; Corvaia, N.; Effenberger, F.; Wolff-Winiski, B.; Krömer, E.; Mudde, G. C. Function and regulation of Fc epsilon RI expression on monocytes from non-atopic donors. *Clin. Exp. Allergy* **1996**, *26*, 630–641.
- Wang, B.; Rieger, A.; Kilgus, O.; Ochiai, K.; Maurer, D.; Födinger, D.; Kinet, J. P.; Stingl, G. Epidermal Langerhans cells from normal human skin bind monomeric IgE via Fc epsilon RI. *J. Exp. Med.* **1992**, *175*, 1353–1365.
- Kikutani, H.; Suemura, M.; Owaki, H.; Nakamura, H.; Sato, R.; Yamasaki, K.; Barsumian, E. L.; Hardy, R. R.; Kishimoto, T. Fc epsilon receptor, a specific differentiation marker transiently expressed on mature B cells prior to isotype switching. *J. Exp. Med.* **1986**, *164*, 1455–1469.
- Vercelli, D.; Jabara, H. H.; Lee, B. W.; Woodland, N.; Geha, R. Human recombinant interleukin-4 induces Fc epsilon R2/CD23 on normal human monocytes. *J. Exp. Med.* **1988**, *167*, 1406–1416.
- Bieber, T.; Rieger, A.; Neuchrist, C.; Prinz, J. C.; Rieber, E. P.; Boltz-Nitulescu, G.; Scheiner, O.; Kraft, D.; Ring, J.; Stingl, G. Induction of Fc epsilon R2/CD23 on human epidermal Langerhans' cells by recombinant interleukin-4 and gamma-interferon. *J. Exp. Med.* **1989**, *170*, 309–314.
- Nacleiro, R. M.; Baroody, F. J. Understanding the inflammatory processes in upper allergic airway disease and asthma. *Allergy Clin. Immunol.* **1998**, *101*, 345–351.
- Maurer, D.; Fiebiger, E.; Ebner, C.; Reininger, B.; Fischer, G. F.; Wichlas, S.; Jouvin, M. H.; Schmitt-Egenolf, M.; Kraft, D.; Kinet, J. P.; Stingl, G. Peripheral blood dendritic cells express Fc epsilon RI as a complex composed of Fc epsilon RI alpha- and Fc epsilon RI gamma-chains and can use this receptor for IgE-mediated allergen presentation. *J. Immunol.* **1996**, *157*, 607–617.
- Mudde, G.; Van Reijssen, C. F. C.; Boland, G. J.; De Gast, G. C.; Bruijnzeel, P. L. B.; Bruijnzeel-Koomen, C. A. F. M. Allergen presentation by epidermal Langerhans' cells from patients with atopic dermatitis is mediated by IgE. *Immunology* **1990**, *69*, 335–341.
- Zhao, G.-D.; Yokoyama, A.; Kohno, N.; Sakai, K.; Hamada, H.; Hiwada, K. Effect of Suplatast Tosilate (IPD-1151T) on a mouse model of asthma: inhibition of eosinophilic inflammation and bronchial hyperresponsiveness. *Int. Arch. Allergy Immunol.* **1999**, *121*, 116–122.
- Tamaoki, J.; Kondo, M.; Sakai, N.; Aoshiba, K.; Tagaya, E.; Nakata, J.; Isono, K.; Nagai, A. Effect of suplatast tosylate, a Th2 cytokine inhibitor, on steroid-dependent asthma: a double-blind randomised study. *Lancet* **2000**, *356*, 273–278.
- Sato, T. A.; Widmer, M. B.; Finkelman, F. D.; Madani, H.; Jacobs, C. A.; Grabstein, K. H.; Maliszewski, C. R. Recombinant soluble murine IL-4 receptor can inhibit or enhance IgE responses in vivo. *J. Immunol.* **1993**, *150*, 2717–2723.
- Maliszewski, C. R.; Sato, T. A.; Davison, B.; Jacobs, C. A.; Finkelman, F. D.; Fanslow, W. C. In vivo biological effects of recombinant soluble interleukin-4 receptor. *Proc. Soc. Exp. Biol. Med.* **1994**, *206*, 233–237.
- Renz, H.; Enssle, K.; Lauffer, L.; Kurrle, R.; Gelfand, E. W. Inhibition of allergen-induced IgE and IgG1 production by soluble IL-4 receptor. *Int. Arch. Allergy Immunol.* **1995**, *106*, 46–54.
- Carballido, J. M.; Schols, D.; Namikawa, R.; Zurawski, S.; Zurawski, G.; Roncarolo, M. G.; deVries, J. E. IL-4 induces human B-cell maturation and IgE synthesis in SCID-hu mice: Inhibition of ongoing IgE production by in vivo treatment with an IL-4/IL-13 receptor antagonist. *J. Immunol.* **1995**, *155*, 4162–4170.
- For a recent review on IL-4 antagonists see the following: Reinemer, P.; Sebald, W.; Duschl, A. The interleukin-4-receptor: from recognition mechanism to pharmacological target structure. *Angew. Chem., Int. Ed.* **2000**, *39*, 2834–2846.
- Renz, H.; Bradley, K.; Enssle, K.; Loader, J. E.; Gelfand, E. W. Prevention of the development of immediate hypersensitivity and airway hyperresponsiveness following in vivo treatment with soluble IL-4 receptor. *Int. Arch. Allergy Immunol.* **1996**, *109*, 167–176.
- Grunewald, S. M.; Werthmann, A.; Schnarr, B.; Klein, C. E.; Bröcker, E. B.; Mohrs, M.; Brombacher, F.; Sebald, W.; Duschl, A. An antagonist IL-4 mutant prevents type I allergy in the mouse: inhibition of the IL-4/IL-13 receptor system completely abrogates humoral immune response to allergen and development of allergic symptoms in vivo. *J. Immunol.* **1998**, *160*, 4004–4009.
- Heusser, C.; Jardieu, P.; Therapeutic potential of anti-IgE antibodies. *Curr. Opin. Immunol.* **1997**, *9*, 805–813.
- Patalano, F. Injection of anti-IgE antibodies will suppress IgE and allergic symptoms. *Allergy* **1990**, *54*, 103–110.
- Coffman, R. L.; Lebman, D. A.; Rothman, P. Mechanism and regulation of immunoglobulin isotype switching. In *Advances in Immunology*; F. J. Dixon, Ed.; Academic Press: San Diego, CA, 1993; Vol. 54, pp 229–270.
- Snapper, C. M.; Marcu, K. B.; Zelazowski, P. The immunoglobulin class switch: beyond "accessibility". *Immunity* **1997**, *6*, 217–223.
- Stavnezer, J. Immunoglobulin Class Switching. *Curr. Opin. Immunol.* **1996**, *8*, 199–205.
- Albrecht, B.; Peiritsch, S.; Woisetschlager, M. A bifunctional control element in the human IgE germline promoter involved in repression and interleukin 4 activation. *Int. Immunol.* **1994**, *6*, 1143–1151.
- Messner, B.; Stütz, A. M.; Albrecht, B.; Peiritsch, S.; Woisetschlager, M. Cooperation of binding sites for STAT6 and NFkB/rel in the interleukin-4 induced upregulation of the human IgE germline promoter. *J. Immunol.* **1997**, *159*, 3330–

3337. Stütz, A. M.; Woisetschläger, M. Functional synergism of STAT6 with either NF-kappaB or PU.1 to mediate IL-4 induced activation of IgE germline gene transcription. *J. Immunol.* **1999**, *163*, 4383–4391.
- (13) Gauchat, J.-F.; Aversa, G. G.; Gascan, H.; De Vries, J. E. Modulation of IL-4 induced germline epsilon RNA synthesis in human B cells by tumor necrosis factor-alpha, anti-CD40 monoclonal antibodies or transforming growth factor-beta correlates with levels of IgE production. *Int. Immunol.* **1992**, *4*, 397–406.
- (14) For recent reviews on PSR/PSQ see the following. Flynn, D. F.; Devraj, R. V.; Parlow, J. J. Recent advances in polymer-assisted solution-phase chemical library synthesis and purification. *Curr. Opin. Drug Discuss. Dev.* **1998**, *1*, 41–50. Booth, R. J.; Hodges, J. C. Solid-Supported Reagent Strategies for Rapid Purification of Combinatorial Synthesis Products. *Acc. Chem. Res.* **1999**, *32*, 18–26.
- (15) Creswell, M. W.; Bolton, G. L.; Hodges, J. C.; Meppen, M. Combinatorial synthesis of dihydropyridone libraries and their derivatives. *Tetrahedron* **1998**, *54*, 3983–3998.
- (16) Calculated with the CMR program, version 3.0, by BioByte Corp., Claremont, CA, 1995.
- (17) Bridges, A. J.; Cody, D. R.; Zhou, H.; McMichael, A.; Fry, D. W. Enantioselective inhibition of the epidermal growth factor receptor tyrosine kinase by 4-(α -phenethylamino)quinazolines. *Bioorg. Med. Chem.* **1995**, *3*, 1651–1656.
- (18) Showalter, H. D. H.; Bridges, A. J.; Zho, H.; Sercel, A. nD.; McMichael, A.; Fry, D. W. Tyrosine Kinase Inhibitors. 16. 6,5,6-Tricyclic enzo[2,3-*d*]pyrimidines and Pyrimido[5,4-*b*]- and -8,4,5-*b*]indoles as Potent Inhibitors of the Epidermal Growth Factor Receptor Tyrosine Kinase. *J. Med. Chem.* **1999**, *42*, 5464–5474.
- (19) Garcia-Echeverria, C.; Traxler, P.; Evans, D. B. ATP Site-Directed Competitive and Irreversible Inhibitors of Protein Kinases. *Med. Res. Rev.* **2000**, *20*, 28–57.
- (20) Esposti, M. D. Inhibitors of NADH-ubiquinone reductase: an overview. *Biochim. Biophys. Acta* **1998**, *1364*, 222–235.
- (21) Gazit, A.; Chen, J.; App, H.; McMahon, G.; Hirth, P.; Chen, I.; Levitzki, A. Tyrphostins IV—highly potent inhibitors of EGF receptor kinase. Structure–activity relationship study of 4-anilidoquinazolines. *Bioorg. Med. Chem.* **1996**, *4*, 1203–1207.
- (22) Blumenkopf, T. A.; Flanagan, M. E.; Brown, M. F.; Changelian, P. S. Preparation of pyrrolo[2,3-*d*]pyrimidines as inhibitors of protein tyrosine kinases such as Janus Kinase 3. PCT Int. Appl. WO 9965909, 1999.
- (23) Halgren, T. A. The Merck Force Field. *J. Comput. Chem.* **1996**, *17*, 490.
- (24) *Jaguar*, versions 3.5 and 4.0; Schrodinger, Inc.: Portland, OR, 1998–1999.
- (25) Slater, J. C. *The Self-Consistent Field for Molecules and Solids*; Quantum Theory of Molecules and Solids, Vol. 4; McGraw-Hill: New York, 1974.
- (26) Vosko, S. H.; Wilk, L.; Nusair, M. Accurate spin-dependent electron liquid correlation energies for local spin density calculations: a critical analysis. *Can. J. Phys.* **1980**, *58*, 1200.
- (27) Becke, A. D. Correlation energy of an inhomogeneous electron gas: a coordinate space model. *Phys. Rev. A* **1988**, *38*, 3098.
- (28) Perdew, J. P. Density-functional approximation for the correlation energy of the inhomogeneous electron gas. *Phys. Rev. B* **1986**, *33*, 8822.
- (29) Mulliken, R. S. Electronic population analysis on LCAO-MO (linear combination of atomic orbitals) wave function (I). *J. Chem. Phys.* **1955**, *48*, 1833.

JM010888H